HUMS2023 Data Challenge Result Submission

Team Name: NRC-AERO-SMPL-01

Team Members: Emma Seabrook, Catherine Cheung

Institutions: National Research Council Canada

Publishable: yes

1. Summary of Findings

Data from DST Group's Planet Gear Fault Propagation test [1] was analysed using anomaly detection and regression machine learning (ML) algorithms. Given data from four vibration channels positioned at four different locations on the gearbox [1], both the crack initiation time as well as the propagation trend for the crack on the planet gear rim were determined. In order to increase the dimensionality of the dataset and provide the machine learning model with more information, gear condition indicators (CI) based on vibration characteristics in the frequency domain were calculated [2], detailed in Section 6.

To detect the point of crack initiation, an ensemble of anomaly detection algorithms were used to find outliers within the data. The algorithms selected files that correspond to anomalies in the gear condition indicators. Since the data point for file 150 aligns with a peak in the condition indicators 'FM0' and 'FM4', we believe that the crack initiated at this point, summarized in Table 1. The trend for crack propagation was generated using a semi-supervised regression ML model. The model was able to produce a regression from a basic training trend and showed that there is a clear trend in crack growth from file 170 which accelerates around file 327. This is consistent with trends in the 'Crest Factor', 'FM0', and 'FM4' condition indicators.

Table 1: Summary of Analysis Results

#	**Detection & Trending**	**Data file name/ number**	**Comments**
1	Consistent detection on at least one signal channel; i.e. the fault indicators remain consistently above the threshold.	#150	Figure 1
2	Confirmed detection on at least two signal channels; i.e. the fault indicators remain consistently above the threshold.	#150	Figure 2
3	Clear multi-channel indication of the characteristic fault features; i.e. faulty planet gear meshing with both the ring and sun gears.	#170	Figure 3 and Figure 4
4	Confirmed trend of fault progression; i.e. a consistent increasing trend started from which file number/name.	#170	Figure 5
5	Confirmed trend of accelerated fault progression; i.e. a consistent exponential increasing trend started from which file number/name	#327	Figure 6

2. Analysis Methods

The analysis was conducted using machine learning models to identify trends and anomalies within the data which are then validated through analysis of the CI trends. Gear condition indicators were calculated and normalized from the time-series data to reveal more information about variations in the vibrations recorded. These condition indicators were the inputs for the anomaly detection and crack growth regression ML models. An ensemble of anomaly detection algorithms were used to extract several points of interest (POI), that is, points that were flagged as anomalies by four or more models. These POIs were then analyzed to see if they could be related to crack propagation. File 150 was determined to be the point of crack initiation by data from sensors IP-1 and XAH-4, while file 170 seemed to be the point at which all of the sensors began to demonstrate a significant variation from the previous trend. The trend forecasting was determined by a semi-supervised machine learning model that was trained on partially-labelled gear CI data and then used to predict the growth of the crack on the full dataset. A fifth-order polynomial fit was then applied to this regression to demonstrate the overall crack growth curve.

3. Illustrating Figures

The following figures illustrate the anomalies detected and trends determined by the ML models.

4. Characteristic Fault Signatures of Early Detection

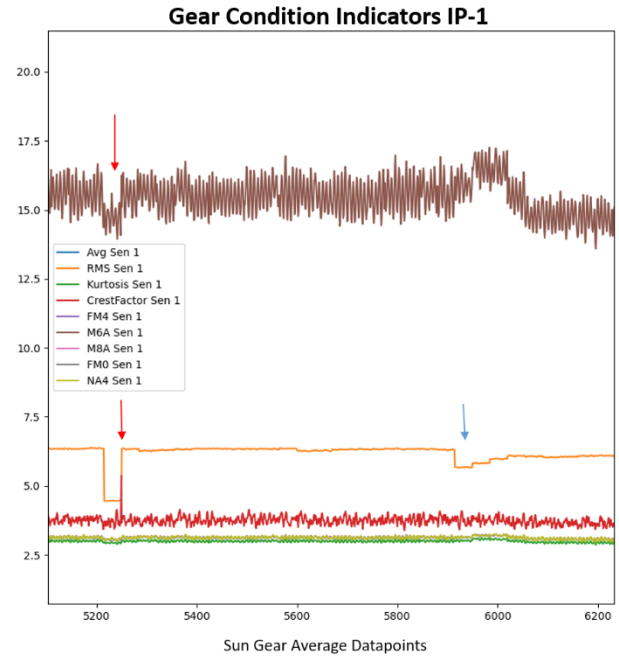

Figure 1: Characteristic fault signal of the earliest detection by channel IP-1 (Sensor 1)

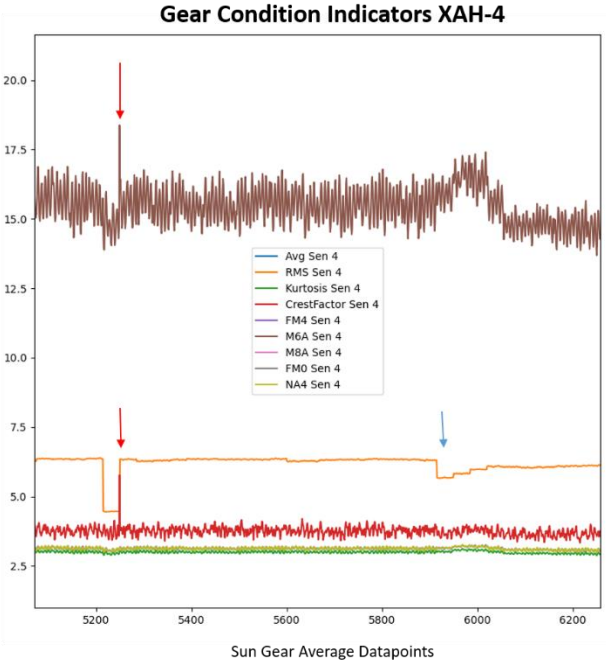

Figure 2: Characteristic fault signal of the earliest detection by channel XAH-4 (Sensor 4)

Figure 1 and Figure 2 above demonstrate the first two indications of a fault at data point 5260 (file 150) marked by the red arrows. This fault is present in channels IP-1 and XAH-4 but not in the other two channels and are characterized by a reduction in the normalized *RMS* for each sensor as well as a peak in the *Crest Factor*. The blue arrows in Figure 1 and Figure 2 indicate a variation in the trend caused by the reduction in speed input to the gearbox at the beginning of a new day of testing and is therefore not considered an anomaly related to crack propagation.

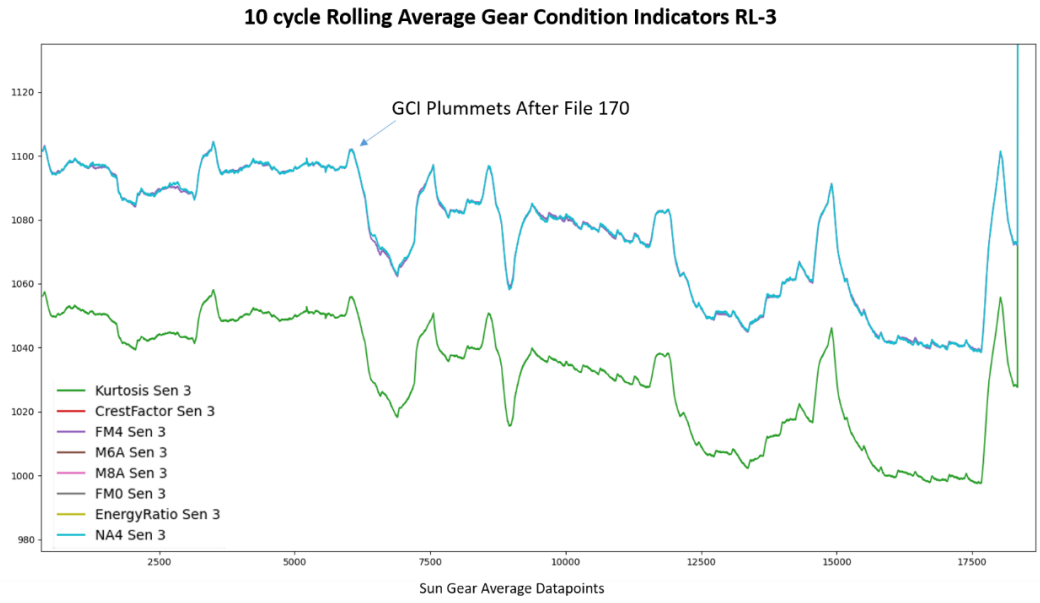

Figure 3: Channel RL-3 (Sensor 3) Kurtosis, NA4, and FM4 Gear Condition Indicators with 10 sun gear revolution rolling average.

Figure 3 demonstrates the point at which the condition indicators begin to show cyclic peaks due to meshing between the sun gear and the cracked planetary gear. These peaks are especially pronounced from points 9000 to 11500 and from 15500 to 17500. Other anomalies present in the plot such as the large valley at point 8500, or the peak at point 15000 are the result of fluctuations in the input torque.

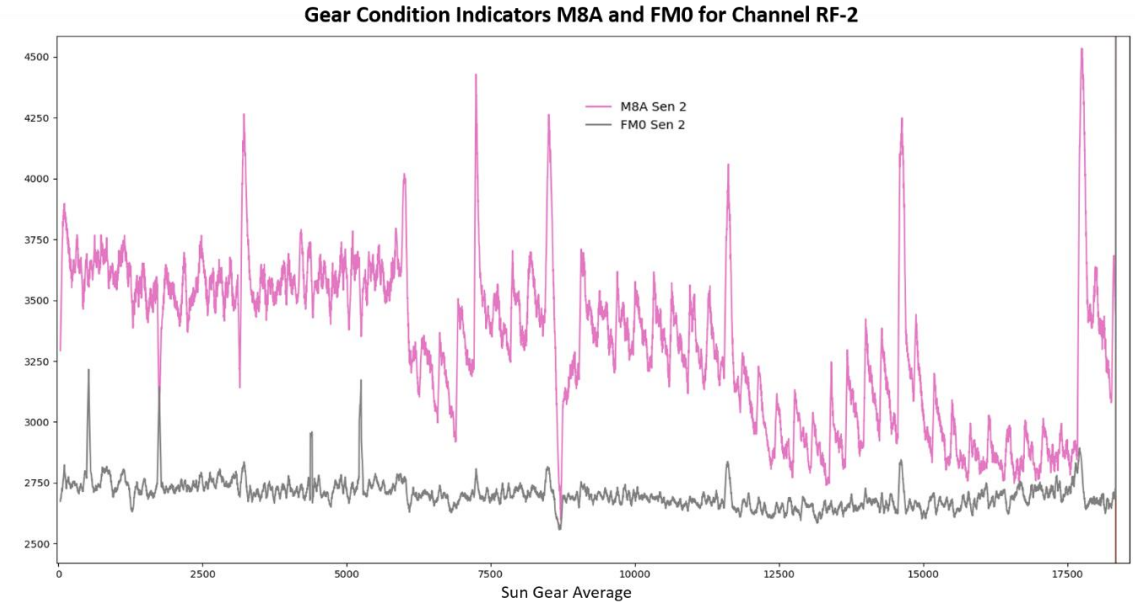

Figure 4: Condition indicators M8A and FM0 for channel RF-2 (Sensor 2)

In Figure 4, we can see the trends in the M8A and FM0 condition indicators for the RF-2 channel. Notably, there is no distinct trend in the M8A indicator before point 6000 (file 171), but after, there is a clear cyclic pattern which is likely the result of the sun gear meshing with the cracked planetary gear tooth. For this reason, it is likely that the crack initiated before file 170.

5. Fault Progression Trending Curve

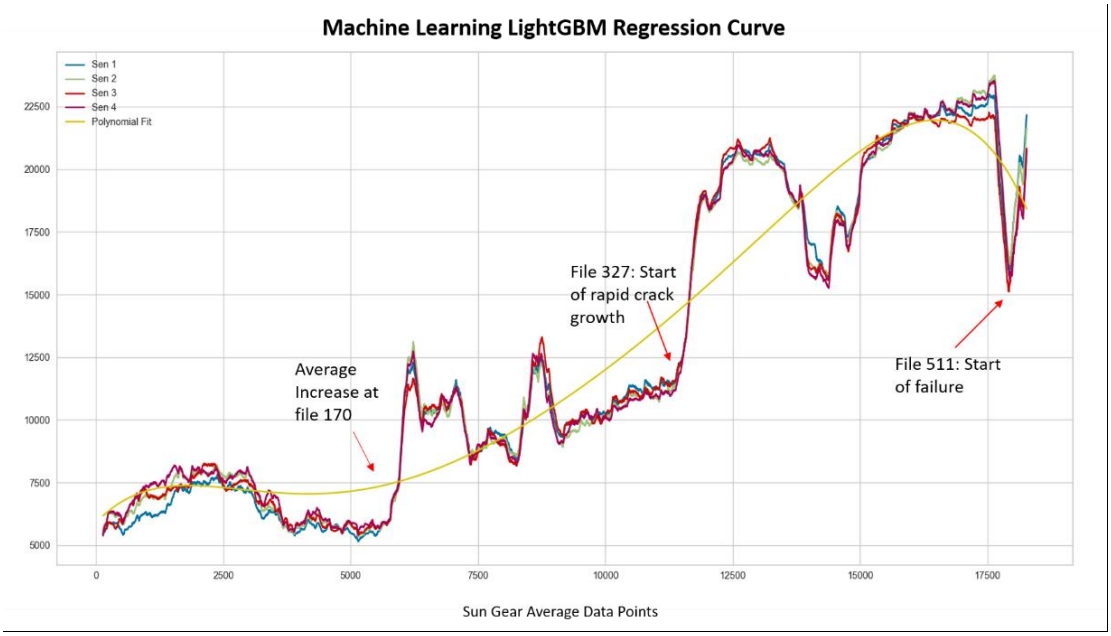

Figure 5: Fault Progression Trending Curve produced by ML regression model: Light Gradient Boosting Machine

The plot in Figure 5 was produced using a Light Gradient Boosting Machine (LightGBM) machine learning model. The model was trained on a basic training trend that had no crack from files 1 to 170, a full crack for files 524 and onward and a linear crack growth trend for the files in between. The trained model was then passed the original (unlabeled) data to generate the crack propagation trend.

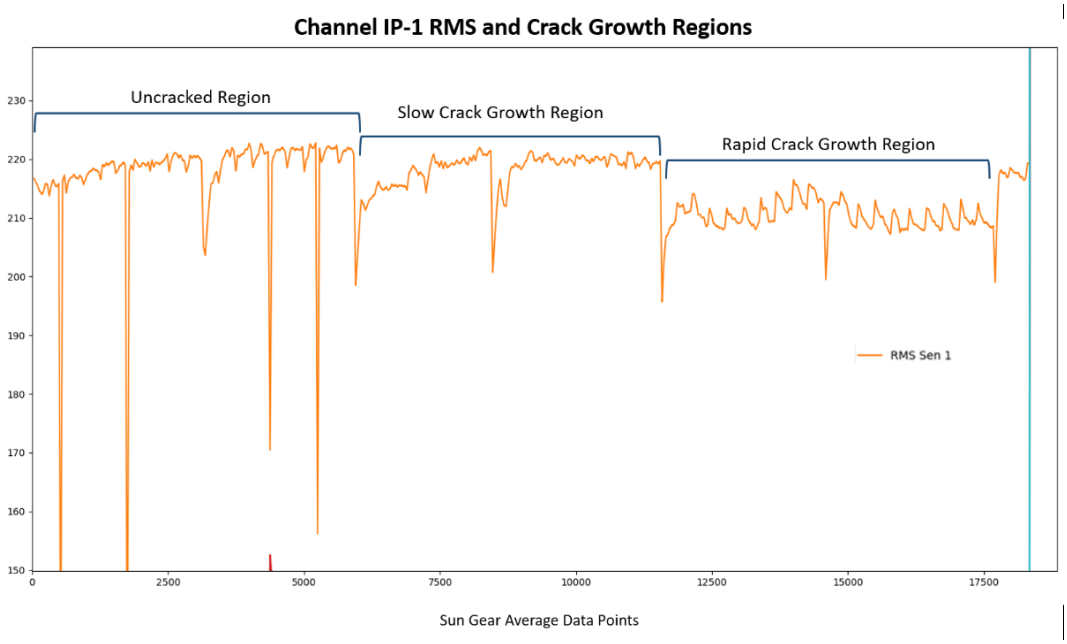

Figure 6: RMS of channel IP-1 (Sensor 1) labeled with crack growth regions.

Figure 6 (above) uses the normalized RMS of the IP-1 channel to illustrate the visual differences in the trends of the gear CIs throughout the different crack growth regimes. The first (un-cracked) region has no discernible pattern beyond the fluctuations in input speed and torque. The second region begins with a

plateau but settles into unsteady variation as the crack grows. The third rapid crack growth region displays consistent cyclic variations characteristic of the increased vibrations resulting from the meshing of the cracked planetary gear.

6. Description of Analysis Methods

The data was analysed in three main steps: data cleaning, dimensionality increase, and machine learning. All three of which were performed using python as well as the Scikit Learn and Pycaret libraries. The first step, data cleaning, involved correcting the data with respect to the input shaft speed and the input torque. This was done by adjusting the data points by a factor of the difference between the shaft speed for that file and the mean shaft speed (≈ 99.988) and equivalently for the input torque (≈ 125.0072) thus reducing any anomalies within the data caused by variation in the input.

Machine learning is a very effective tool to help analyze data especially when the data is highly dimensional. In this dataset, there were only four sensor measurements, so to increase the dimensionality of the data and to extract patterns that would otherwise be difficult to distinguish in the time domain, gear condition indicators were calculated and normalized. The chosen indicators were: *Root Mean Square, Kurtosis, Crest Factor, FM0, FM4, M6A, M8A, Energy Ratio and NA4* and were chosen based on recommendations made by [3]. These indicators vary with the frequency, phase, and amplitude of the data making them a good signal for when a dataset, especially one with constant cyclic data such as gear vibration data, strays from the norm. According to [3], the best condition indicators for this case are *FM0*, and *FM4* for wear and bending due to root crack as well as Kurtosis and Crest Factor for breakage, wear, and impulse vibrations respectively.

The gear CIs are calculated from three variations of the data signal called the Time Synchronous Average (TSA), Regular, Residual, and Difference signals. The regular signal is composed of the primary frequency of the TSA along with its first-order sidebands. The residual signal is the TSA signal with the harmonics removed while the difference signal additionally has the regular signal and first-order sidebands removed.

The formulas for the gear condition indicators are as follows [4, 5, 6]:

$$RMS = \sqrt{\frac{1}{N}[\sum_{i=1}^{n}(x_i)^2} \qquad CrestFactor = \frac{x_o - peak}{RMS} \qquad Kurtosis = \frac{N\sum_{i=1}^{N}(x_i-\bar{x})^4}{(\sum_{i=1}^{N}(x_i-\bar{x})^2)^2}$$

$$Energy\ Ratio = \frac{RMS_d}{RMS_{reg}} \qquad FM0 = \frac{P2P_x}{\sum_{N=0}^{H} P_N} \qquad FM4 = Kurtosis(difference)$$

$$M6A = \frac{N^2\sum_{i=1}^{N}(d_i-\bar{d})^6}{(\sum_{i=1}^{N}(d_i-\bar{d})^2)^3} \qquad M8A = \frac{N^2\sum_{i=1}^{N}(d_i-\bar{d})^8}{(\sum_{i=1}^{N}(d_i-\bar{d})^2)^4} \qquad NA4 = \frac{N\sum_{i=1}^{N}(r_{iM}-\bar{r}_M)^6}{\frac{1}{M}\sum_{j=1}^{M}(\sum_{i=1}^{N}(r_{ij}-\bar{r}_j)^2)^2}$$

Description of fault detection method

The fault was detected using a combination of analytical and anomaly detection machine learning methods. The gear CIs were calculated for each revolution of the sun gear to produce 18410 data points. These gear CIs along with the mean amplitude of that revolution of the sun gear were then passed through several anomaly detection machine learning algorithms that extracted numerous anomalies. The various models frequently identified anomalies in files 150, 158, and 173 for channel IP-1, files 159 and 161 in channel RF-2, 179 in channel RL-3, and 171 in channel XAH-4. Further investigation revealed a spike in the Crest Factor and a dip in the RMS of IP-1 and XAH-4 data at file 150, as shown in Figure 1 and Figure 2; however, this anomaly was not present for RF-2 and RL-3. Moreover, there was a significant change in

the trend at point 170 across all sensors, illustrated in Figure 3, whereas before that point, the only variance in the data was due to the changes in input speed at the end of each day of data collection. However, after file 170, there is a clear cyclic trend in the data that peaks every hunting tooth cycle (Figure 4). This peak is likely a result of the sun gear meshing with the fault in the planetary gear thus demonstrating that the crack must have initiated prior to file 170 and validating that the anomaly at file 150 was likely the beginning of the crack.

Description of fault trending method

A semi-supervised regression machine learning algorithm was used to determine the fault trend by training a machine learning model on partially labelled data with a basic linear trend applied to it and then using that same model to predict a trend on each sensor's data. This was tested using a variety of machine learning model types including a linear regression, bagging regression, clustering regression, and gradient boosting regression models. Although they all produced slightly different trends, the trends consistently displayed three regions with distinct amplitude differences: the un-cracked region, the slow crack growth region, and the rapid crack growth region as can be seen in Figure 5. In Figure 6, we can see these same categories presented with the rolling averaged RMS condition indicator where the first region (un-cracked) has only minor cyclic variations that remain fairly constant throughout. The large dips in this region are due to variations in the input speed and the smaller reduction in RMS is the result of the speed reduction at the beginning of the day. The second region immediately has a plateau where there is very little variation but then sees a significant sudden increase around data point 7000 (file 200). The remainder of this region has very little variation aside from the decrease resulting from the start-of-day speed increase, but overall, the mean RMS of this region is lower than that of the previous one. The third, rapid crack growth region, has an even lower average RMS and also exhibits regular cyclic peaks likely due to the sun gear meshing with the planetary gear crack. These cyclic peaks have a period of approximately one hunting tooth cycle which validates that they are being caused by the fault.

Using anomaly detection and regression machine learning (ML) methods to identify anomalies and trends in the gear CIs, the crack initiation time was determined to be at file 150, the crack growth trend was determined to begin at file 170, and the trend was determined to accelerate around file 327.

7. Supplemental Information

[1] W. Wang, D. Blunt and J. Kappas, *Helicopter main gearbox planet gear crack propagation test dataset: A description of the dataset for HUMS 2023 data challenge,* Melbourne: Defence Science and Technology Group (DST Group), 2022.

[2] P. M. K. a. R. Š. Večeř, "Condition indicators for gearbox condition monitoring systems," *Acta Polytechnica,* vol. 45, no. 6, pp. aa-bb, 2005.

[3] A. P. Vikas Sharma, "A Review of Gear Fault Diagnosis Using Various Condition Indicators," *Procedia Engineering,* vol. 144, pp. 253-263, 2016.

[4] J. J. Zakrajsek, "An investigation of gear mesh failiure prediction techniques," Cleveland State University, Cleveland, 1989.

[5] J. Zakrajsek, D. P. Townsend and H. J. Decker, "An Analysis of Gear Fault Detection Methods as Applied to Pitting Fatigue Failure Data," NASA, Cleveland, OH, 1993.

[6] J. A. Keller and P. Grabill, "Vibration monitoring of UH-60A main transmission planetary carrier fault," in *Annual Forum Proceedings - American Helicopter Society*, Phoenix, AZ, 2003.